

Comparison of Hydrogen Adsorption on Diamond and Graphite Surfaces

Hiroaki NAKAMURA^{1,2)}, Atsushi M. ITO¹⁾, Seiki SAITO²⁾, Yuichi TAMURA³⁾,
Susumu FUJIWARA⁴⁾, Noriyasu OHNO²⁾ and Shin KAJITA⁵⁾

¹⁾National Institute for Fusion Science, 322-6 Oroshi-cho, Toki 509-5292, Japan

²⁾Department of Energy Engineering and Science, Graduate School of Engineering, Nagoya University,
Nagoya 464-8603, Japan

³⁾Konan University, 8-9-1 Okamoto, Higashinada-ku, Kobe 658-8501, Japan

⁴⁾Kyoto Institute of Technology, Matsugasaki, Sakyo-ku, Kyoto 606-8585, Japan

⁵⁾EcoTopia Science Institute, Nagoya University, Nagoya 464-8603, Japan

(Received 6 December 2009 / Accepted 11 March 2010)

By a classical molecular dynamics (CMD) simulation with a modified Brenner's reactive empirical bond-order (REBO) potential, we found that graphite with zigzag (10 $\bar{1}$ 0) and armchair (11 $\bar{2}$ 0) edge states is destroyed more easily than other structures, i.e., graphite with the (0001) surface, and diamond with the (100), (111), (120), and (110) surfaces. Experimental results indicated that graphite is eroded under hydrogen atom injection with $E_{in} = 0.3$ eV, and that diamond is not eroded under the same conditions. Our simulation results are consistent with these experimental results. We also reveal the temperature and saturation dependence of the surface structure of carbon crystals.

© 2010 The Japan Society of Plasma Science and Nuclear Fusion Research

Keywords: molecular dynamics simulation, graphite, edge state, zigzag, armchair, diamond, sputtering, hydrogen, carbon, surface structure

DOI: 10.1585/pfr.5.S2072

1. Introduction

Carbon material is popular for use in the walls of plasma equipment. For example, carbon fiber composite (CFC) is used in divertor plates in the Large Helical Device (LHD) [1]. The mechanism for hydrocarbon yield by plasma-wall interaction is an interesting topic for many researchers [1–5].

Recently, two of the authors (N. Ohno and S. Kajita) presented the results of an experiment on chemical sputtering of diamond and graphite by hydrogen plasma [6–8]. They investigated the carbon erosion in a detached plasma with a weight loss method using the toroidal divertor plasma simulator NAGDIS-T (NAGoya DIvertor plasma Simulator with Toroidal magnetic configuration) [9].

As the target in their experiment, they used two carbon materials, an isotropic graphite sample and a polycrystalline diamond composite sample. They measured the weight loss of the samples under a detached hydrogen plasma, the injection energy of which was estimated as 0.3 eV [6, 8]. They found that weight loss occurs in the graphite sample at temperatures from 600 to 800 K. They also found that the weight loss of the diamond sample was almost zero. They concluded that diamond has greater strength against hydrogen injection than graphite.

We have been developing a simulation method to reveal the plasma-wall interaction mechanism using a classi-

cal molecular dynamics (CMD) simulation of interactions between hydrogen and graphite by the modified Brenner's reactive empirical bond-order potential (REBO) model [10–12],

In our previous studies, which examined hydrogen injection onto the surface of either graphene or graphite, we qualitatively obtained the injection energy dependence of the hydrogen adsorption ratio due to graphene or graphite [12–19]. Moreover, the dynamics of the adsorption process was also revealed by observing the motion of hydrogen and carbon atoms.

In a recent paper [20], we chose diamond as a material composed of carbon atoms. Using a CMD simulation, we revealed the time dependence of adsorption on diamond with four different surfaces: the (100), (111), (120), and (110) surfaces. We also found that chemical sputtering does not occur when the injection hydrogen energy E_{in} is less than 5 eV.

In this paper, we investigate qualitatively the dependence of chemical sputtering on the surface structure of diamond and graphite. We use a CMD simulation of three different graphite surface structures and four different diamond surface structures.

The main difference between diamond and graphite is the crystal structure [21]. Graphite is composed of graphene sheets, interlayers of which interact with each other by a weak potential, the van der Waals interaction

author's e-mail: hnakamura@nifs.ac.jp

potential. Bonds between the carbons of each graphene sheet are sp^2 covalent bonds. In contrast, the carbons of diamond are linked by an sp^3 covalent bond. Covalent bonds have a stronger attractive force than van der Waals interaction bonds. By intuitive analysis, therefore, diamond is expected to have greater strength against hydrogen injection than graphite. This expectation agrees with experimental results [6–8]. We investigate qualitatively the dependence of chemical sputtering on the surface structure of diamond and graphite by a CMD simulation in this paper.

2. Simulation Method

2.1 Simulation algorithm

To investigate the kinetic processes of carbon and hydrogen, we use the CMD algorithm with a modified Brenner's reactive empirical bond order (REBO) potential that we proposed to investigate chemical reactions between hydrogen and graphene in previous simulations [10–19].

Second-order symplectic integration [22] is used to solve the time evolution of the equation of motion. The time step is 5×10^{-18} s. The modified Brenner's REBO potential [10, 11] has the form:

$$U \equiv \sum_{i,j>i} \left[V_{[ij]}^R(r_{ij}) - \bar{b}_{ij}(\{r\}, \{\theta^B\}, \{\theta^{DH}\}) V_{[ij]}^A(r_{ij}) \right], \quad (1)$$

where r_{ij} is the distance between the i -th and the j -th atoms. The functions $V_{[ij]}^R$ and $V_{[ij]}^A$ represent repulsion and attraction, respectively. The function \bar{b}_{ij} generates a multi-body force. The bond angle θ_{jik}^B is the angle between the vector from the i -th atom to the j -th atom and the vector from the i -th atom to the k -th atom. The dihedral angle θ_{kijl}^{DH} is the angle between the plane passing through the j -th, i -th, and k -th atoms and the plane passing through the i -th, j -th, and l -th atoms. The parameters $\{r\}$, $\{\theta^B\}$, and $\{\theta^{DH}\}$ denote all sets of r_{ij} , θ_{jik}^B , and θ_{kijl}^{DH} , respectively (see the details of the modified Brenner's REBO potential in Ref. [17]).

2.2 Simulation model

2.2.1 Structure of the target

The simulation model is shown in Fig. 1. We simulate seven different carbon structures [20]:

- Case 1: Graphite with the (0001) surface (Fig. 1)
- Case 2: Graphite with the (10 $\bar{1}$ 0) surface, i.e., zigzag edge state (Fig. 2 (a))
- Case 3: Graphite with the (11 $\bar{2}$ 0) surface, i.e., arm-chair edge state
- Case 4: Diamond with the (100) surface (Fig. 3 (a))
- Case 5: Diamond with the (111) surface
- Case 6: Diamond with the (120) surface
- Case 7: Diamond with the (110) surface

The center of mass of the diamond is set as the origin of the coordinates. The xyz coordinates are defined in

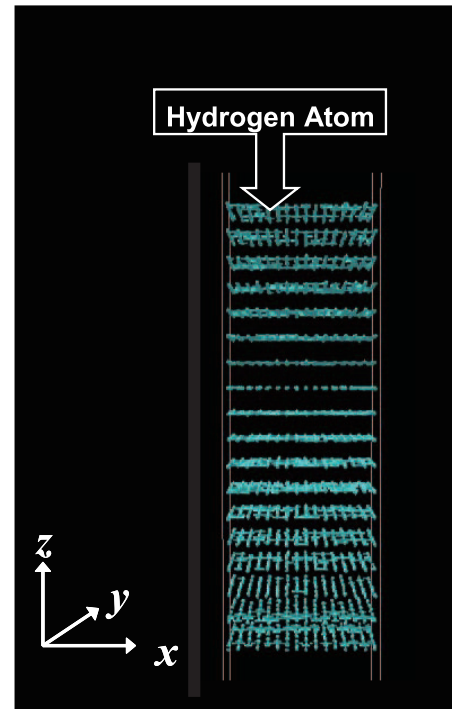


Fig. 1 (color online) Simulation model. We define the x -, y -, and z -axes as seen here. Figure is drawn for graphite with the (0001) surface, one of seven simulated in this paper. Hydrogen atoms are injected individually from above, parallel to the z -axis.

Fig. 1, and a periodic boundary condition is applied in the x and y directions. All carbon structures have no lattice defects and no crystal edges due to these periodic boundary conditions. The velocity of carbon atoms in graphene in the initial state corresponds to the Maxwell distribution function with a temperature of 300 K.

2.2.2 Hydrogen injection

Hydrogen atoms are injected individually onto the carbon surface parallel to the z -axis from $z = 0.4$ nm. The x and y coordinates of the injection position of each hydrogen are set at random. The kinetic energy of all injected hydrogens E_{in} is set to 0.3 eV.

3. Simulation Results

3.1 Temperature of carbon crystal

We show the temperature of each carbon crystal for $E_{in} = 0.3$ eV in Fig. 4. When the simulation time becomes about 20 ps, the temperature of the diamond is saturated without increasing, even though hydrogen atoms continue to be injected to the diamond. For graphite, the temperature of the two edge states, i.e., (10 $\bar{1}$ 0) and (11 $\bar{2}$ 0), increases more than that of the (0001) state and the diamond states. The reason for this property will be discussed in Section 4.

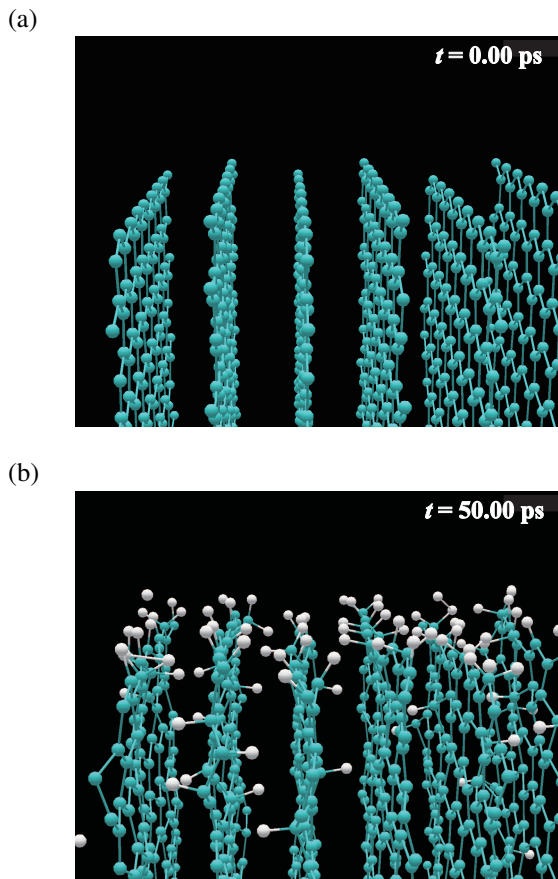


Fig. 2 (color online) Surface structures of graphite with zigzag edge state (Case 2). (a) Initial configuration of graphite with (10 $\bar{1}0$) surface, i.e., zigzag edge state. Each graphene is slanted toward the next nearest sheet (AB stacking structure). (b) When hydrogen injection begins and continues for 50 ps, hydrogen atoms enter the graphite crystal. Thus, the crystal structure begins to be destroyed. White and green balls denote hydrogen and carbon, respectively.

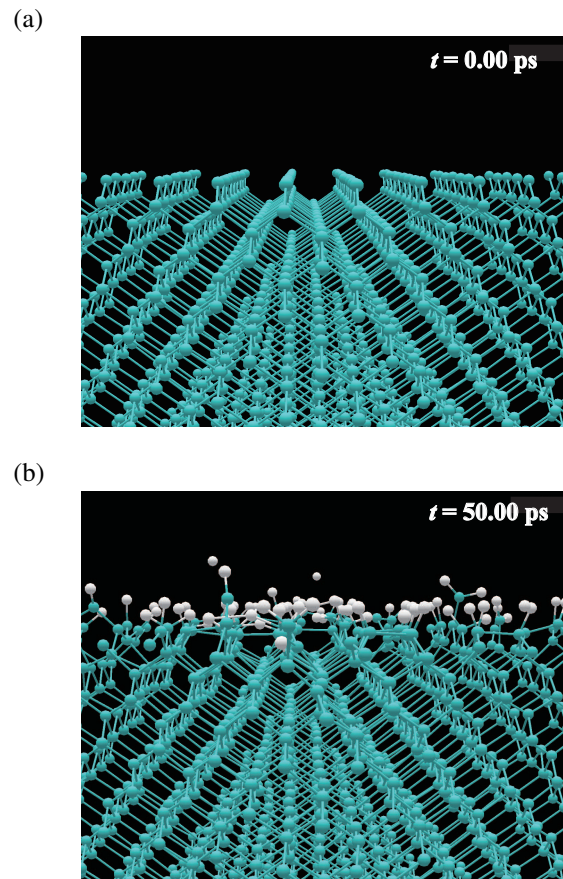


Fig. 3 (color online) Surface structures of diamond with (100) surface (Case 4). (a) Initial configuration of diamond with (100) surface. (b) When hydrogen injection begins and continues for 50 ps, hydrogen atoms are adsorbed on the surface of the diamond. In contrast to graphite (Fig. 2), hydrogen does not enter the bulk of the diamond. Therefore, the diamond structure is not destroyed. White and green balls denote hydrogen and carbon, respectively.

3.2 Hydrogen coverage rate

We also measure the hydrogen coverage rate over the surface of a carbon crystal, as shown in Fig. 5. For diamond, the shape of the curve of the coverage rate is similar to that in Fig. 4. However, the time dependence of the coverage rate of diamond is clearer than that of the temperature. Figures 2 (b) and 5 reveal that it is easy for hydrogen atoms to enter graphite with the armchair and zigzag edge states. This agrees with the intuitive consideration of the configuration of graphite with these two edge states. In graphite with these two edge states, the spaces between graphene sheets are exposed to hydrogen injection. Hydrogen, therefore, enters graphite more easily than it does diamond. However, graphite with the (0001) surface and diamond prevent ingress of hydrogen into the bulk of the crystal. Their coverage rates, therefore, are saturated with time.

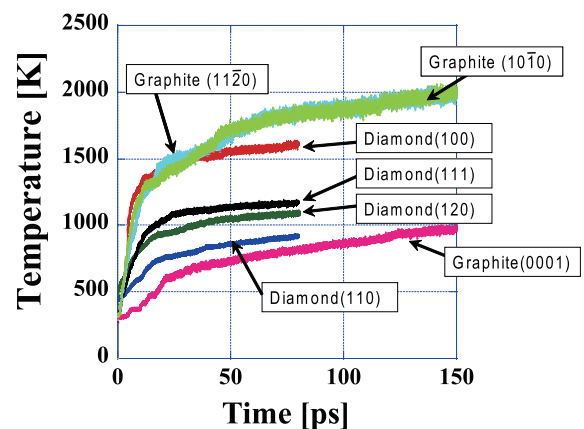


Fig. 4 (color online) Temperature of each carbon crystal. In graphite with zigzag and armchair edge states, the temperature increases. In contrast, the temperature is saturated for graphite with the (0001) surface and diamond. The saturated temperature depends on the surface structure [20].

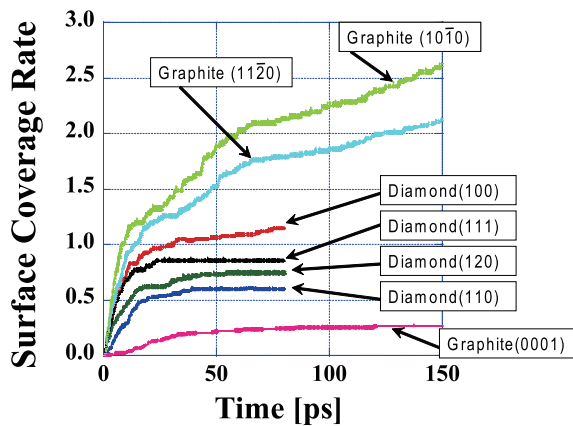


Fig. 5 (color online) Time dependence of the hydrogen coverage rate for each carbon crystal surface structure. Coverage rates for graphite with zigzag and armchair edge states increase without saturation.

4. Discussion and Conclusion

From the simulation results in Section 3, we found that graphite with the zigzag and armchair edge states is destroyed more easily than the other structures, i.e., graphite with the (0001) surface and diamond. Experimental results [6–8] indicated that graphite is eroded under hydrogen atom injection with $E_{in} = 0.3$ eV, and that diamond is not eroded under the same conditions. Our simulation results are consistent with these results except for the behavior of graphite with the (0001) surface. This inconsistency is explained as follows: In our simulation, graphite with the (0001) surface is regarded as a borderless plane with no edges and no defects because we adopt a periodic boundary condition. A previous work has shown that ideal graphite with the (0001) surface has great strength against hydrogen injection with low injection energy [16]. However, the graphite sample used in the experiment is not a simple crystal but a polycrystalline graphite. Therefore, it has edge states or defects. This is a reason why the simulation result for graphite with the (0001) surface is not consistent with the experimental result. We will be expanding our simulation code to treat larger carbon structures. If it becomes possible to treat polycrystalline graphite structures, the inconsistency should be eliminated in the future.

Acknowledgment

This work was supported by the National Institutes of Natural Sciences undertaking Forming Bases for Interdisciplinary and International Research through Cooperation Across Fields of Study and Collaborative Research

Program (No. NIFS09KEIN0091), and by a Grants-in-Aid for Scientific Research (No. 19055005) from the Ministry of Education, Culture, Sports, Science and Technology, Japan.

- [1] A. Sagara, S. Masuzaki, T. Morisaki, S. Morita, H. Funaba, M. Goto, Y. Nakamura, K. Nishimura, N. Noda, M. Shoji, H. Suzuki, A. Takayama, A. Komori, N. Ohyabu, O. Motojima, K. Morita, K. Ohya, J. P. Sharpe and LHD Experimental Group, *J. Nucl. Mater.* **313-316**, 1 (2003).
- [2] T. Nakano, H. Kubo, S. Higashijima, N. Asakura, H. Takemura, T. Sugie and K. Itami, *Nucl. Fusion* **42**, 689 (2002).
- [3] J. Roth, *J. Nucl. Mater.* **266-269**, 51 (1999).
- [4] J. Roth, R. Preuss, W. Bohmeyer, S. Brezinsek, A. Cambe, E. Casarotto, R. Doerner, E. Gauthier, G. Federici, S. Higashijima, J. Hogan, A. Kallenbach, A. Kirschner, H. Kubo, J. M. Layet, T. Nakano, V. Philipps, A. Pospieszczyk, R. Pugno, R. Ruggieri, B. Schweer, G. Sergienko and M. Stamp, *Nucl. Fusion* **44**, L21 (2004).
- [5] B. V. Mech, A. A. Haasz and J. W. Davis, *J. Nucl. Mater.* **241-243**, 1147 (1997).
- [6] N. Ohno, presented at the 11th ITPA meeting on SOL/divertor physics, September 15-18, Nagasaki, Japan, 2008.
- [7] K. Yada, N. Matsui, N. Ohno, S. Kajita, S. Takamura and M. Takagi, *J. Nucl. Mater.* **390-391**, 290 (2009).
- [8] K. Yada, M. S. thesis, Dept. Energy and Science, Nagoya Univ., Nagoya, Japan, 2009.
- [9] M. Nagase, H. Masuda, N. Ohno, S. Takamura and M. Takagi, *J. Nucl. Mater.* **363-365**, 611 (2007).
- [10] D. W. Brenner, *Phys. Rev. B* **42**, 9458 (1990) [Erratum; *ibid* **46**, 1948 (1992)].
- [11] D. W. Brenner, O. A. Shenderova, J. A. Harrison, S. J. Stuart, B. Ni and S. B. Sinnott, *J. Phys. Condens. Matter* **14**, 783 (2002).
- [12] A. Ito and H. Nakamura, *Commun. Comput. Phys.* **4**, 592 (2008).
- [13] A. Ito and H. Nakamura, *J. Plasma Phys.* **72**, 805 (2006).
- [14] H. Nakamura and A. Ito, *Mol. Sim.* **33**, 121 (2007).
- [15] A. Ito and H. Nakamura, *Thin Solid Films* **516**, 6553 (2008).
- [16] A. Ito and H. Nakamura, *Jpn. J. Appl. Phys.* **47**, 4715 (2008).
- [17] A. Ito, H. Nakamura and A. Takayama, *J. Phys. Soc. Jpn.* **77**, 114602 (2008).
- [18] A. Ito, Y. Wang, S. Irle, K. Morokuma and H. Nakamura, in Proceedings of the 22nd IAEA Fusion Energy Conference, Geneva, Switzerland, October 13-18, 2008, TH/7-1.
- [19] H. Nakamura, A. Takayama and A. Ito, *Contrib. Plasma Phys.* **48**, 265 (2008).
- [20] H. Nakamura, A. M. Ito, S. Saito, A. Takayama, Y. Tamura, N. Ohno and S. Kajita, accepted for publication in *Jpn. J. Appl. Phys.* (2010).
- [21] A. C. Ferrai and J. Robertson, *Phys. Rev. B.* **61**, 14095 (2000).
- [22] M. Suzuki, *J. Math. Phys.* **26**, 601 (1985).